IFASD 2015
International Forum on Aeroelasticity and Structural Dynamics
June 28 — July 02, 2015 ▲ Saint Petersburg, Russia

Bifurcation Analysis of the Aeroelastic Galloping Problem via Input-Output Parametric Modelling

Nicholas F. Giannelis[1] **and Gareth A. Vio**

School of Aeronautical, Mechanical and Mechatronic Engineering
Building J11, The University of Sydney, NSW, 2006, Australia

[1]e-mail: nicholas.giannelis@sydney.edu.au

Keywords: Aeroelastic Galloping, System Identification, NARMAX

Abstract. This paper explores the bifurcation behaviour of the aeroelastic galloping system through an input-output parametric modelling. The models are trained with periodic output data and parametrised with respect to flow velocity and initial condition. Comparisons to numerical integration find that while the system identification routine can accurately predict limit cycle amplitudes, a divergence in long term simulation error persists.

1 INTRODUCTION

The past two decades have seen a substantial increase in the interest of non-linear problems within the aeroelastic research community. This research has been primarily focused on the development of full unsteady coupled Computational Fluid Dynamic-Finite Element (CFD-FE) solutions of complex aeroelastic problems. Much less attention has been given to fundamental solutions of simple, non-linear aeroelastic systems. However, owing to the large computational cost of coupled CFD-FE simulations, the work in this field has been mainly focused on obtaining system responses, with little research on the classification of complex non-linear behaviour. Conversely, fundamental investigations of simple aeroelastic systems have seen significant developments regarding stability prediction, bifurcation analysis and low cost approximate solutions. As such, there exists a need of extending the methodologies developed for conducting stability analysis on fundamental aeroelastic systems to more complex configurations without the prohibitive computational overhead.

The aeroelastic cross-wind galloping problem, described by the steady flow over a square cylinder spring-mass-damper, provides an example of a fundamental aeroelastic system that presents complex nonlinear behaviour. The quasi-steady theory for this system was first developed by Parkinson and Brooks [1], where a fifth order polynomial damping nonlinearity was introduced to describe the aerodynamic force. This formulation was extended by Parkinson and Smith [2], where seventh order polynomial damping was included to permit the presence of hysteresis. Experimental validation of the analytic expression was provided by Norberg [3], where a dependency between Reynolds number and hysteresis was observed. Vio *et. al.* [4] have considered a variety of techniques in exploring the bifurcation behaviour of the aeroelastic galloping system. The methods of Harmonic Balance, Cell Mapping, Higher Order Harmonic Balance, Centre Manifold linearisation, Normal Form and numerical continuation were examined, with varying success in predicting the full response spectrum. Nonetheless, no attempt has been made at identifying the non-linear system from either simulation or experimental data.

Common practise in aeroelastic system identification dictates the use of Proper Orthogonal Decomposition (POD) in the development of Reduced Order Models (ROMs) [5]. Whilst these

ROMs typically perform well within the sample space from which they have been constructed, extensions to conditions outside of this space are not robust. Input-output parametric models developed under a Nonlinear AutoRegressive Moving Average with eXogenous variables (NARMAX) methodology have also seen applicability in aeroelastic systems [6]. The identified models are, however, prone to divergence from the true system as the technique offers no constraint on long term simulation error.

Several recent publications [7–9] have explored the use of Expectation Maximisation and Particle Filter techniques as a means of identifying non-linear systems exhibiting autonomous oscillations. Whilst promising results are seen in predicting complex neuron spiking dynamics, the technique appears to suffer a similar divergence in long term simulation error. A recently developed method for non-linear system identification that explicitly addresses the simulation error bounds has been proposed by Manchester *et. al.* [10]. The Transverse Robust Identification Error (TRIE) formulates the system identification routine as a convex optimisation problem, and has seen excellent results in the prediction of Limit Cycle Oscillations (LCOs) in the dynamics of live rat neuron membranes.

In this paper, we present preliminary findings in the applicability of the NARMAX methodology in predicting LCO behaviour of the aeroelastic galloping system. The mathematical model describing the true system representation is provided under variable damping levels. The NARMAX formulation is presented and with the applicable aspects of the algorithm given in detail. A description of the numerical integration procedure for the galloping problem is then provided, along with classification of the bifurcation characteristics across various velocities and initial conditions. The identified model is employed to predict the LCO and bifurcation behaviour of the system and performance is evaluated against the predictions of the numerical integration. A future study will evaluate the efficacy of the Particle Filter and TRIE techniques in identification of the aeroelastic galloping system.

2 MATHEMATICAL MODEL

The aeroelastic galloping system considered here is modelled as a mass with linear stiffness and non-linear damping as shown in Figure 1. The model is a prism of length l, mass m, square cross-section of height h and is suspended from a linear spring of stiffness k and a linear damper with a damping coefficient of c.

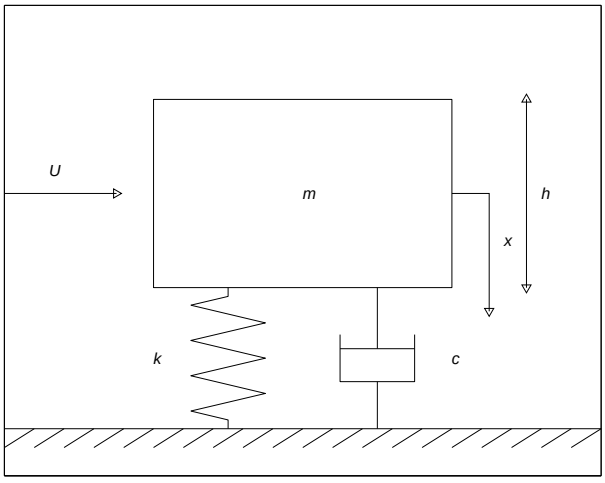

Figure 1: Aeroelastic Galloping Model

The aerodynamic force provides the non-linear damping, as given by:

$$mx'' + cx' + kx = \frac{1}{2}\rho U^2 C_F(\tau) hl \tag{1}$$

where ρ is the air density, U is the airspeed, ($'$) denotes differentiation with respect to time, τ, and the aerodynamic force coefficient, $C_F(\tau)$, is expressed as a polynomial function of velocity:

$$C_F = \left(A\frac{x'}{U} - B\left(\frac{x'}{U}\right)^3 + C\left(\frac{x'}{U}\right)^5 - D\left(\frac{x'}{U}\right)^7 \right) \tag{2}$$

In this expression $A = 2.69$, $B = 168$, $C = 6270$ and $D = 59900$ were obtained empirically by Parkinson and Smith [2] through curvefitting experimental results. After non-dimensionalising, Equation 1 becomes:

$$\ddot{y} + y = nA\left(\left(V - \frac{2\beta}{nA}\right)\dot{y} - \left(\frac{B}{AV}\right)\dot{y}^3 + \left(\frac{C}{AV^3}\right)\dot{y}^5 - \left(\frac{D}{AV^5}\right)\dot{y}^7\right) \tag{3}$$

where $y = x/h$, $n = \rho h^2 l/(2m)$, V is the non-dimensional airspeed given by $V = U/(\omega h)$, $\beta = c/(2m\omega)$, $\omega = \sqrt{k/m}$ and ($\dot{}$) represents differentiation with respect to the non-dimensional time $t = \omega\tau$. This provide the complete aeroelastic galloping equation of motion, which when expressed in compact form becomes:

$$\ddot{y} + y = f(\dot{y}) \tag{4}$$

where

$$f(\dot{y}) = nA\left(\left(V - \frac{2\beta}{nA}\right)\dot{y} - \left(\frac{B}{AV}\right)\dot{y}^3 + \left(\frac{C}{AV^3}\right)\dot{y}^5 - \left(\frac{D}{AV^5}\right)\dot{y}^7\right) \tag{5}$$

In this study two cases will be considered

- Case 1: Low damping. $\beta = 1.07 \times 10^{-3}$ yields a critical velocity $V_c = 1.85$. This value of β was used in an experimental investigation by [2].
- Case 2: High damping. $\beta = 0.5$, which corresponds to $c = m\omega$, yields a critical velocity $V_c = 864.53$

The critical velocity is obtained by equating the linear damping term in Eq. (3) to zero.

$$V_c = \frac{2\beta}{nA} \tag{6}$$

The response of the system at non-dimensional airspeeds below V_c is decaying. At supercritical speeds the system undergoes LCOs, with amplitudes that depend on airspeed and initial conditions.

3 NARMAX FORMULATION

3.1 Power-Form Polynomial Representation

Identification of the aeroelastic galloping system is performed under the NARMAX methodology developed by Leontartis and Billings [11], with the relevant aspects of the algorithm provided below. The model is defined by:

$$y_k = F^{(l)}(y_{k-1}, ..., y_{k-n_y}; u_{k-1}, ..., u_{k-n_u}; e_{k-1}, ..., e_{k-n_e}) + e_k \tag{7}$$

where $y(k)$, $u(k)$ and $e(k)$ are the system output, input and noise signals respectively; n_y, n_u and n_e are the maximum regressions for the system output, input and noise; $F(\cdot)$ is some non-linear function and l is the degree of non-linearity. The identification problem of the galloping system inherently reduces to determining a non-linear function, $F(\cdot)$, from a set of basis functions that is able to capture the varying amplitude autonomous oscillations. The basis functions considered here are power-form polynomials, such that Equation 7 may be represented as the sum of each of the model terms:

$$y(k) = \sum_{i=1}^{n_\theta} \theta_i p_i(k) + e(k) \tag{8}$$

where $p_i(k)$ are the model terms or regressors, θ_i are the model coefficients and n_θ is the total number of terms. The system identification routine is integrated in two concurrent steps, namely, the selection of significant model terms and parameter estimation. A Forward Regression (FR) is employed for model order selection and an Orthogonal Least Squares (OLS) is used for parameter estimation, comprising the FROLS algorithm of Billings *et. al.* [12].

For the basic OLS estimator, the factorisation of Equation 8 is transformed into a regression model with orthogonal model terms, such that:

$$y(k) = \sum_{i=1}^{n_\theta} g_i w_i(k) + e(k) \tag{9}$$

where $w_i(k)$ are orthogonal over the training data sets and g_i are the corresponding coefficients. The FR algorithm begins by considering all possible process terms $p_i(k)$ (dictated by the imposed maximum lags n_y, n_u and n_e) as candidates for the first model term. Each process term is considered orthogonal in this initial term selection, such that:

$$\boldsymbol{w}_m^{(1)} = \boldsymbol{p}_m \tag{10}$$

where $\boldsymbol{w}_m^{(1)}$ is the m^{th} candidate for the first orthogonal model term, $\boldsymbol{p}_m$ is the m^{th} regressor inclusive of all data samples and $m = 1, 2, ..., M$ where M is the total number of candidate model terms. The estimated coefficients of these first model terms, $g_m^{(1)}$ are then determined through the OLS estimator:

$$g_m^{(1)} = \frac{\boldsymbol{y}^T \boldsymbol{w}_m}{\boldsymbol{w}_m^T \boldsymbol{w}_m} \tag{11}$$

where the training set, $\boldsymbol{y}$ is taken to be the final 1000 points of simulation data calculated through numerical integration at each condition. The significance of each candidate term is to the model output is then evaluated through computation of the Error Reduction Ratio (ERR):

$$ERR^{(1)}(m) = \left(g_m^{(1)}\right)^2 \frac{\boldsymbol{w}_m^T \boldsymbol{w}_m}{\boldsymbol{y}^T \boldsymbol{y}} \tag{12}$$

where $ERR^{(1)}(m)$ represents the incremental increase in explained variance of the output $\boldsymbol{y}$ introduced by the inclusion of the orthogonal vector $\boldsymbol{w}_m$ to the model. The first model term l_1 is selected such that it provides the highest degree of explanatory significance:

$$l_1 = arg \max_{l \leq m \leq M} \{ERR^{(1)}(m)\} \tag{13}$$

For selection of the subsequent model terms, the first base is removed from the candidate dictionary of regressors and an orthogonal transformation is applied to the remaining candidates according to:

$$\boldsymbol{w}_m^{(s)} = \boldsymbol{p}_m - \sum_{r=1}^{s-1} \frac{\boldsymbol{p}_m^T \boldsymbol{w}_r}{\boldsymbol{w}_r^T \boldsymbol{w}_r} \boldsymbol{w}_r \tag{14}$$

The calculations proceed as per Equations 11-13 for the s^{th} significant model terms. The algorithm terminates once the sum of incrementally explanatory variance exceeds a predefined threshold value C_d (set to 99.99% for the computations in this paper):

$$\sum_{s=1}^{M_0} ERR(s) \geq C_d \tag{15}$$

where M_0 is the number of model terms yielding an explanatory variance of C_d. It is important to note that as the NARMAX methodology is being employed to identify a system exhibiting autonomous oscillations, the system inputs are non-existent, and as such will not appear in the identified models. Further, in this preliminary study, true simulation data is employed for model selection and parameter estimation. A noise model will be integrated in a future study, where experimental validation will be sought.

3.2 Common Model Structure Selection

The algorithm outlined in Section 3.1 will potentially identify a different model structure for each of the conditions considered. Ideally, a common model structure will be determined to describe the LCO behaviour of the galloping system, with the model coefficients parametrised by velocity and initial condition. Derived from the standard FROLS algorithm, Wei *et. al.* [13] have developed a Common Model Structure Selection (CMSS) algorithm for such a purpose. In this model the fidelity of each individual fit is sacrificed such that a common model may capture the LCO behaviour across a range of conditions.

The procedure for CMSS essentially follows that of the preceding section, however, the algorithm is now run over all the output data sets across the range of non-dimensional velocities and

initial conditions considered. Let $\boldsymbol{\phi}_{j,m}$ denote the m^{th} basis vector of the j^{th} test condition. The ERR selection criteria is applied across the total number of test conditions L, such that:

$$ERR^{(1)}(j,m) = \frac{\left(\boldsymbol{y}^T\boldsymbol{\phi}_{j,m}\right)^2}{\left(\boldsymbol{y}^T\boldsymbol{y}\right)\left(\boldsymbol{\phi}_{j,m}^T\boldsymbol{\phi}_{j,m}\right)} \tag{16}$$

The significant terms in the model are then selected according to the average ERR across all test conditions:

$$l_1 = arg\max_{l\leq m\leq M}\left\{\frac{1}{L}\sum_{j=1}^{L} ERR^{(1)}(j,m)\right\} \tag{17}$$

The computations proceed according to Equation 14 and 15, with modification to the basis vectors such that each test condition is considered.

In this study, the CMSS algorithm is applied to the low damping galloping case to parametrise the NARMAX coefficients as a function of non-dimensional velocity and initial condition. The functions are curve-fit from the NARMAX coefficients and take the form:

$$\boldsymbol{g}_j = \begin{cases} \boldsymbol{f}(V_j) & \textit{for Initial Amplitude } < \textit{ 0.5} \\ \boldsymbol{h}(V_j) & \textit{otherwise} \end{cases} \tag{18}$$

where $\boldsymbol{g}_j$ is a vector of length equal to the number of significant terms identified by the CMSS algorithm and $\boldsymbol{f}(\cdot)$ and $\boldsymbol{h}(\cdot)$ are vector polynomial functions of non-dimensional velocity V with degree 7. Although this factorisation will invariably degrade the fidelity of the NARMAX fit for each individual test condition, it permits a compact representation of the complex system behaviour across the entire test space.

4 NUMERICAL INTEGRATION

To determine the true behaviour of the galloping system and provide training data sets for the system identification routine, numerical integration of Equation 3 is performed. In this work, the non-linear equation of motion is realised in MATLAB and Simulink, with the native ODE5 routine performing integration through the explicit fixed-step Runge-Kutta (4,5) scheme, the Dormand-Prince pair [14].

Due to the low damping forces present in Case 1, significant simulation time is required before steady state, autonomous oscillations are observed. This computational effort is reduced by seeding the first test point at $V = 1.86$ with an initial condition of similar order to the LCO amplitude determined by Vio *et. al.* [4]. Subsequent test points are seeded with the LCO amplitude of the preceding condition. A physical time step of $\Delta t = 0.1$ seconds with 2^{15} simulation points is found to be sufficient to observe steady state oscillations. An analogous procedure is employed for numerical integration of the high damping condition, with $\Delta t = 0.03$ seconds and 2^{16} simulation points required to observe LCOs across all test points.

The extensive analysis of the aeroelastic galloping system conducted by Vio *et. al.* [4] found that regardless of the damping level or non-dimensional velocity, the system exhibits symmetric Period-1 LCOs. This greatly simplifies the computation of the LCO amplitude and period, where the amplitude is simply the maximum response once the system has achieved steady

state and the period is obtained from the time-lapse between two consecutive zero crossings of the displacement $y(t)$ in the positive y direction.

For representation of the global stability behaviour of the galloping system across a range of airspeeds and initial conditions, time responses provide limited insight. Rather, bifurcation diagrams, which give the LCO amplitude as a function of non-dimensional velocity, are considered. In Figure 2, the bifurcation plots are provided for both the low and high damping cases.

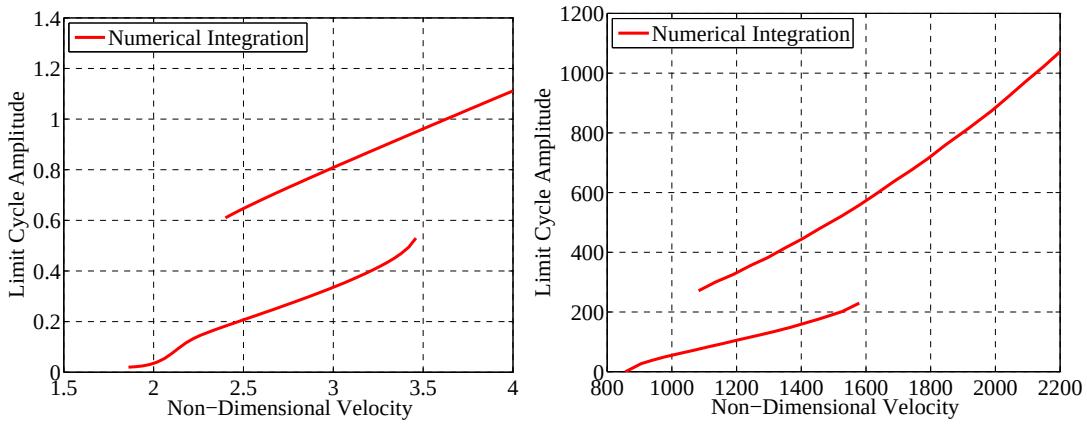

(a) Low Damping (b) High Damping

Figure 2: Bifurcation Diagrams for the Aeroelastic Galloping System

In the low damping case of Figure 2(a), at non-dimensional airspeeds below $V_c = 1.85$, the response of the system is decaying and the limit cycle amplitude is zero. At speeds between 1.85 and 2.4 the system undergoes LCOs with increasing amplitude. At speeds between 2.4 and 3.5 two LCO amplitudes coexist. The system may approach either of these LCOs depending on the initial conditions. This indicates the presence of an unstable limit cycle between these two solutions. At speeds higher than 3.5 there is again only one possible limit cycle. In the high damping case of Figure 2(b), at non-dimensional airspeeds below $V_c = 864.53$ the response of the system is decaying and the limit cycle amplitude is zero. At speeds between V_c and 1090 the system undergoes LCOs with increasing amplitude. At speeds between 1090 and 1560 two LCO amplitudes exist. At speeds higher than 1560 there is again only one possible limit cycle.

The presence of two coexisting limit cycles within a range of airspeeds indicates a hysteric loop in the bifurcation behaviour of the aeroelastic galloping system. This sensitivity to initial conditions necessitates multiple simulations at equivalent airspeeds to completely capture the hysteretic loop within the system. This complex bifurcation behaviour complicates the system identification routine, as the identified model must be capable of capturing both bifurcation branches.

5 RESULTS

NARMAX identification of the low damping galloping system in autonomous oscillation yields a very simplistic model across all non-dimensional velocities and initial conditions. A linear auto-regressive model is determined in each case, with the model terms represented by the first and second lag of displacement y. This simple model structure is expected from the galloping system, where symmetric Period-1 limit cycles are present at all conditions. The corresponding bifurcation diagram for the low damping case is given in Figure 3. When an individual NARMAX fit is applied to each data set, an excellent prediction of the LCO amplitude is observed.

Conversely, the CMSS results exhibit discrepancies relative to the numerical integration, particularly towards the extremities of non-dimensional velocity. The polynomial fit of the coefficients diverges near the first fold point and drifts from the true response amplitude at higher velocities. Nonetheless, the polynomial fit performs well near the second fold point where the bifurcation plot is predominantly linear, and the parametrised model is able to predict the LCO amplitude with a fair degree of accuracy for the majority of the conditions considered.

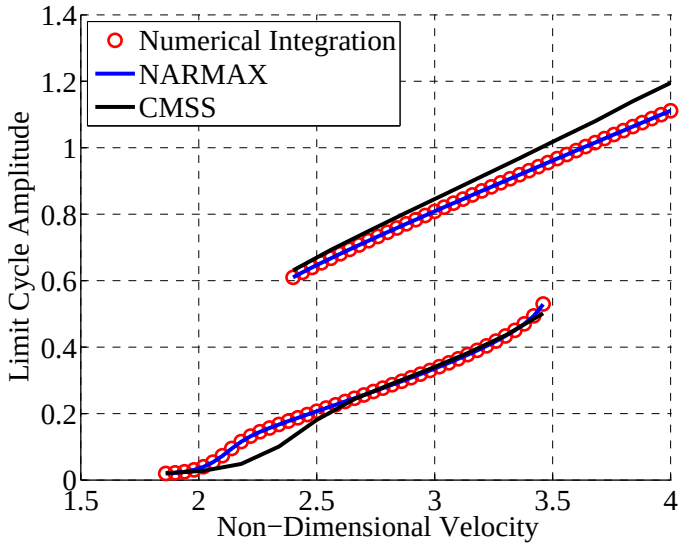

Figure 3: Bifurcation Diagram - Low Damping

Although the amplitudes of the autonomous oscillations are well predicted for the low damping case, NARMAX models are prone to divergence in long-period simulation error. This attribute of the NARMAX method presents itself in the current work, where the predicted LCO frequency diverges from the true response. In Figure 4(a), the initial tracking of the NARMAX model for the lower bifurcation branch at $V = 2.5$ is given. Excellent correlation is observed relative to the numerical integration. However, as simulation time progresses a phase shift in the response develops, as evident in the phase change observed in Figure 4(b).

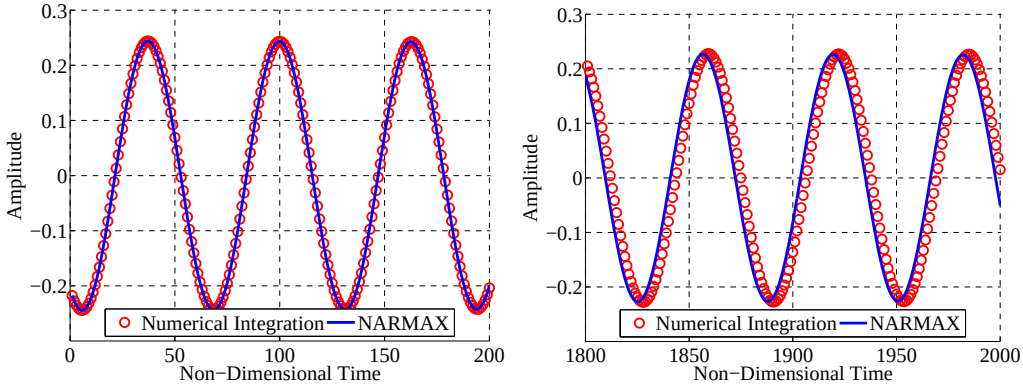

(a) Initial Tracking (b) Long-Period Tracking

Figure 4: Time Responses for NARMAX Model - $V = 2.5$

The inaccuracy in LCO frequency prediction is exacerbated in the CMSS model response of Figure 5(a). Seeded with initial conditions drawn directly from the numerical integration, the

model predicted LCO diverges in phase from the outset, whilst the amplitude remains well captured. This long term divergence in simulation error is a pertinent issue in identification of non-linear systems exhibiting autonomous oscillations. A possible means of alleviation is by use of the TRIE technique of Manchester *et. al.* [10], where the model is derived directly through minimisation of simulation error.

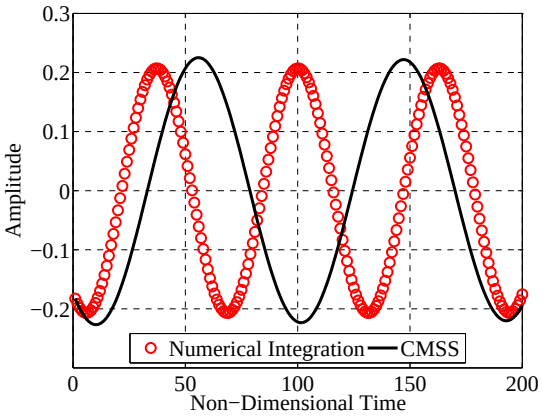

Figure 5: Time Response for CMSS Model - $V = 2.5$

The resultant bifurcation diagram for the high damping case is given in Figure 6. The lower branch amplitudes are well captured by the NARMAX models, where again a linear auto-regressive model structure is selected comprising of two lagged output terms. This is to be expected as the lower branch exhibits near constant frequency LCOs, with similar behaviour to the low damping case. Application of the NARMAX method to the upper branch, however, yields diverging results in the predicted LCO amplitudes. At velocities above $V = 1900$, higher order terms are included in the identified model, which result in unstable oscillations. The upper branch of the high damping case represents a more complex identification problem, as the LCO frequency varies near quadratically with velocity. Accurate representation of this upper branch through a NARMAX routine may necessitate an extension of the basis functions considered during the model selection.

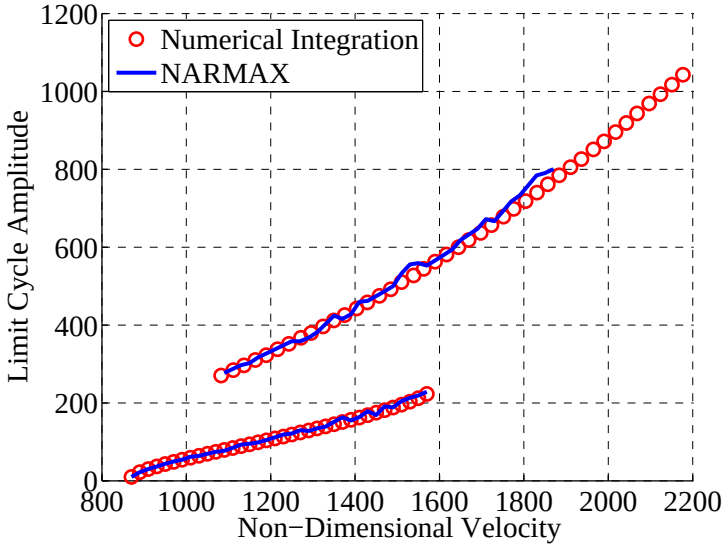

Figure 6: Bifurcation Diagram - High Damping

6 CONCLUSIONS

In this paper, a NARMAX system identification routine has been shown to be effective at predicting LCO amplitudes and bifurcation behaviour in the lightly damped aeroelastic galloping system. Parametrisation of the model coefficients to obtain a common model structure yielded fair amplitude predictions across the range of velocities and initial conditions considered. Simple, linear auto-regressive parametric models were identified as sufficient in determining the low damping magnitudes of autonomous oscillation. However, the routine did highlight a shortcoming in the use of such parametric models, namely, divergence in the long term simulation error. Further, the method employed in this study did not completely capture the bifurcation behaviour of the high damping case. A continuation of this work will consider extensions of the NARMAX modelling, as well as comparisons of the NARMAX identified models against Particle Filter and the TRIE techniques.

REFERENCES

[1] P. Parkinson and N.P.H. Brooks. On the aeroelastic instability of bluff cylinders. *Journal of Applied Mechanics*, 28(2):252–258, 1961.

[2] P. Parkinson and J.D. Smith. The square prism as an aeroelastic non-linear oscillator. *Quarterly Journal of Mathematical and Applied Mathematics*, 17(2):225–239, 1964.

[3] C. Norberg. Flow around rectangular cylinders: pressure forces and wake frequencies. *Journal of Wind Engineering and Industrial Aerodynamics*, 49(1):187–196, 1993.

[4] G.A. Vio, G. Dimitriadis, and J.E. Cooper. Bifurcation analysis and limit cycle oscillation amplitude prediction methods applied to the aeroelastic galloping problem. *Journal of Fluids and Structures*, 23(7):983–1011, 2007.

[5] D.J. Lucia, P.S. Beran, and W.A. Silva. Reduced-order modeling: new approaches for computational physics. *Progress in Aerospace Sciences*, 40(1):51–117, 2004.

[6] S.L. Kukreja and M.J. Brenner. Nonlinear aeroelastic system identification with application to experimental data. *Journal of guidance, control, and dynamics*, 29(2):374–381, 2006.

[7] A. Wills, T.B. Schön, and B. Ninness. Parameter estimation for discrete-time nonlinear systems using Expectation Maximisation. In *Proceedings of the 17th IFAC World Congress, Seoul, Korea*, pages 1–6, 2008.

[8] T.B. Schön, A. Wills, and B. Ninness. System identification of nonlinear state-space models. *Automatica*, 47(1):39–49, 2011.

[9] J. Nordh, T. Wigren, T.B. Schön, and B. Bernhardsson. Particle filtering based identification for autonomous nonlinear ODE models. In *Proceedings of the 17th IFAC Symposium on System Identification (SYSID)*. Beijing, China, October, 2015.

[10] I.R. Manchester, M.M. Tobenkin, and J. Wang. Identification of nonlinear systems with stable oscillations. In *Decision and Control and European Control Conference (CDC-ECC), 2011 50th IEEE Conference on*, pages 5792–5797. IEEE, 2011.

[11] I.J. Leontaritis and S.A. Billings. Input-output parametric models for non-linear systems part I: deterministic non-linear systems. *International journal of control*, 41(2):303–328, 1985.

[12] S.A. Billings, M.J. Korenberg, and S. Chen. Identification of non-linear output-affine systems using an orthogonal least-squares algorithm. *International Journal of Systems Science*, 19(8):1559–1568, 1988.

[13] H.L. Wei, Z.Q. Lang, and S.A. Billings. Constructing an overall dynamical model for a system with changing design parameter properties. *International Journal of Modelling, Identification and Control*, 5(2):93–104, 2008.

[14] J.R. Dormand and P.J. Prince. A family of embedded Runge-Kutta formulae. *Journal of computational and applied mathematics*, 6(1):19–26, 1980.

COPYRIGHT STATEMENT